JOURNAL OF MATERIALS SCIENCE 26 (1991) 4945–4952

Chemical vapour deposition of silicon onto iron: influence of silicon vapour phase source on the composition and nature of the coating

C. KLAM, J.-P. MILLET, H. MAZILLE
LPCI, Bât. 401, INSA, 69621 Villeurbanne Cedex, France
J. M. GRAS
Department of Material Study, EDF, Les Renardières, 77250 Moret-sur-Loing, France

Armco iron was siliconized with two different gas mixtures in the temperature range of 750 to 1100 °C. The Ar–SiH_4–H_2 mixture leads mainly to the formation of a non-porous and adherent solid solution with a maximum silicon content of 6% by weight. For high concentrations of silane in the vapour phase or low treatment temperatures, non adherent pure silicon powder or flakey iron silicides may also depose. The use of Ar–SiH_4–$SiCl_4$–H_2 mixture leads to the immediate nucleation of Fe_3Si, the growth of which occurring from and around the open porosity of the coating. The influence of various parameters such as vapour phase composition and flow rate, hydrogen dilution and treatment temperature, is investigated and analysed in terms of limiting factors of the overall process: gas phase transport, interfacial reactions and diffusion velocity of different species in solid phase.

1. Introduction

A great variety of protective coatings have been developed to improve the oxidation or corrosion behaviour of metallic materials in aggressive environment. For instance, surface enrichment of steel substrates with silicon is well-known to increase their chemical resistance either in hot oxidizing atmospheres [1–4] or in some corrosive solutions [5, 6]. The chemical vapour deposition of silicon has been proposed in the past few years, as one of the most convenient method [7–13]. Because of the large range of deposition conditions and due to various chemical reactions resulting from different sources of silicon used for the vapour phase, a large diversity of coating properties can be obtained.

The use of argon-tetrachlorosilane (Ar–$SiCl_4$) gaseous mixture in equilibrium with solid silicon leads to adherent deposit of iron-silicide Fe_3Si (14.35 wt %), the thickness and porosity of which depend on chosen treatment parameters [5, 10]. According to previous work, the porosity results from the exchange mechanism between the deposited silicon and the iron coming out in the form of $FeCl_2$, volatile at the treatment temperature [8]. It is also attributed to the difference of diffusion coefficient between iron and silicon into the iron silicide layer [13, 14]. Such a porosity is a serious limitation for wide acceptance of siliconizing process for corrosion applications.

The aim of this work was to investigate various treatment conditions in order to obtain a thick, adherent coating with low porosity. Two kinds of gaseous phase were used as silicon source: either argon-tetrasilane-hydrogen mixture (Ar–SiH_4–H_2) or argon-tetrasilane-tetrachlorosilane-hydrogen mixture (Ar–SiH_4–$SiCl_4$–H_2). The specific effect of $SiCl_4$ on the structural properties of the diffusion layer is examined to shed light on the deposition reaction mechanism and to determine the structure and the growth rate of the deposited layers with both silicon sources.

2. Experimental procedure

2.1. CVD process

Armco iron is used as substrate. Its composition is given in Table I. Samples to be treated are chemically polished in an oxalic acid-hydrogen peroxide aqueous solution. Their shape (thick-wall tube: outer diameter 12 mm; inner diameter 7 mm; length 5 to 10 mm) allows to position them onto a silica glass tubing inside a silica glass reactor at a siliconizing temperature varying between 750 and 1100 °C (Fig. 1).

A previous annealing treatment of two hours at 800 °C in pure hydrogen is carried out before introducing the siliconizing gaseous phase. For the argon-tetrasilane-hydrogen mixture, commercially available Ar–3%SiH_4 gas is used and adequately diluted with pure hydrogen or pure argon. Hydrogen is preferred as a gas carrier, to avoid the undesirable oxidation effects on coating nucleation and growth, and to slow down the decomposition rate of silane and

TABLE I Composition (wt %) of Armco iron

C	Si	Mn	P	S	Cu	Ni	O
0.03	0.003	0.03	0.009	0.023	0.01	0.09	0.075

0022–2461/91 $03.00 + .12 © *1991 Chapman & Hall*

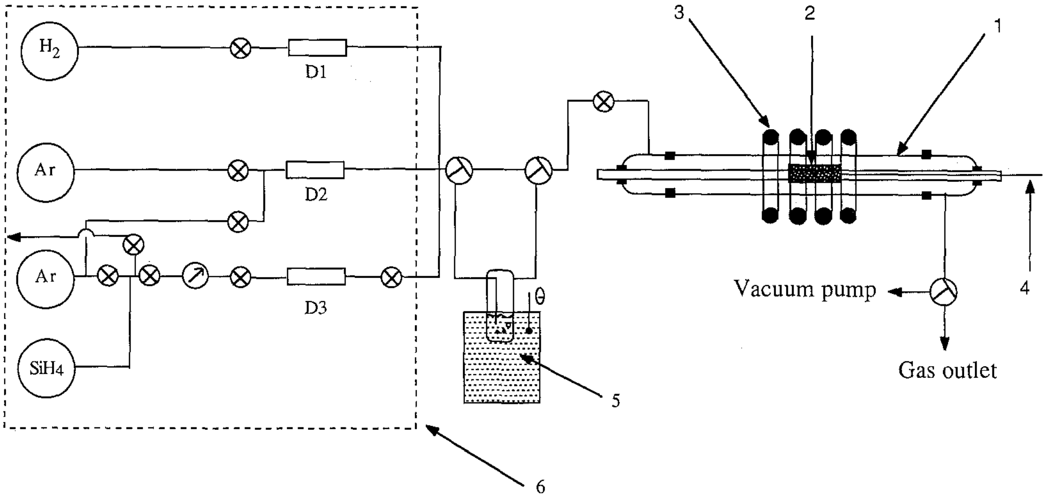

Figure 1 Flow system and apparatus used for the siliconizing process. Key: 1. silica glass reactor, 2. sample for treatment, 3. induction coil, 4. thermocouple, 5. $SiCl_4$ saturator, and 6. gas distribution panel and flowmeters (D).

so minimize the heterogeneous gas phase nucleation of silicon. Hydrogen is also necessary to bring out the reduction of silicon halide in the case of silicon tetrachloride containing mixture. The second mixture is obtained by bubbling argon or argon–3% silane in a saturator containing silicon tetrachloride. The control of the saturator temperature allows the control of $SiCl_4$ vapour pressure and therefore the final composition of the siliconizing atmosphere.

The thermal instability of tetrasilane requires a direct heating of the substrate, using a classic RF furnace and the sample as a susceptor. The power of the generator is carefully adjusted by continuously controling the sample temperature during the CVD treatment.

2.2. Examination

The structure and the composition of the obtained coatings are analysed by X-ray diffraction and secondary ionic mass spectroscopy (SIMS). Incident ions are oxygen ions. Optical and scanning electron microscopies (SEM), electronic microprobe observations, as well as Vickers microhardness measurements are made on previously polished cross-sectioned samples.

3. Results

3.1. Ar–SiH_4–H_2 mixture

3.1.1. Composition and structure of the coatings

Whatever the experimental parameters (gas composition and flow rate, duration and temperature of treatment. . .), the siliconizing treatment always leads to the formation of a non-porous and adherent solid solution with a maximum silicon content of 6% by weight at the outer surface. Only the use of high concentration of silane in the vapour phase allows the formation and deposit of pure silicon powder or flakes of silicon-rich iron silicides such as Fe_5Si_3 or FeSi. That mainly occurs at lowest investigated temperatures. Pure silicon or iron silicides are non-adherent and disjoin from the underlying solid solution during the cooling down at the end of the treatment.

Figure 2 corresponds to the cross-section of the coating obtained after a one hour treatment at 1000 °C and Fig. 3 is relative to the silicon depth profile of the same coating, determined by electronic microprobe analysis. The checking of the true surface composition, by using previously chemically analysed bulk iron-silicon alloys, confirms that the silicon amount does not exceed 11 at % (6% by weight) and regularly decreases up to the substrate.

The cross-section metallography in Fig. 4, with microhardness determinations reported in Fig. 5, corresponds to a two hours siliconized sample at 1100 °C. The hardness increases in the solid solution, from the substrate to the surface of the treated sample up to 300 $Hv_{0.1}$, that is about three times harder than for non-treated Armco iron. These values are in good agreement with Mitani *et al.* [15] data obtained on bulk iron-silicon alloys with similar silicon content.

The distribution profiles of Si^+_{28}, Fe^+_{56} and Fe^+_{84} ionic species determined by secondary ionic mass

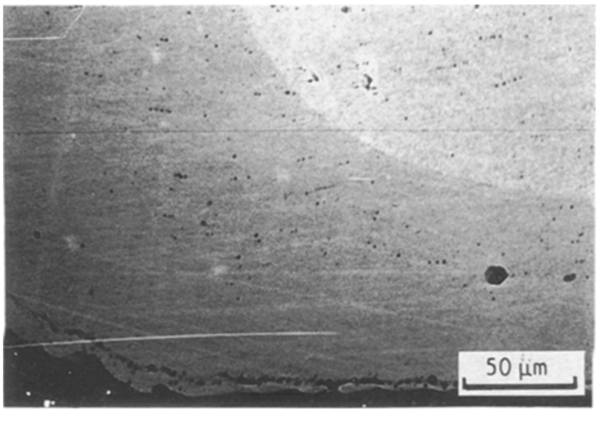

Figure 2 Backscattered electrons image of a cross-section of a siliconized sample after one hour CVD treatment at 1000 °C (total gas flow rate: 1.75 l h^{-1}; Ar 22.2 vol %; SiH_4 0.7 vol %; H_2 77.1 vol %).

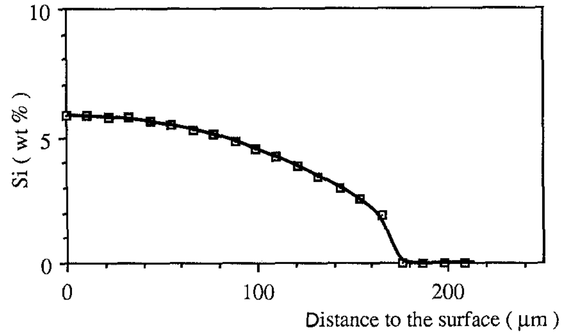

Figure 3 Distribution profile of silicon (wt %) into the coating determined by microprobe analysis.

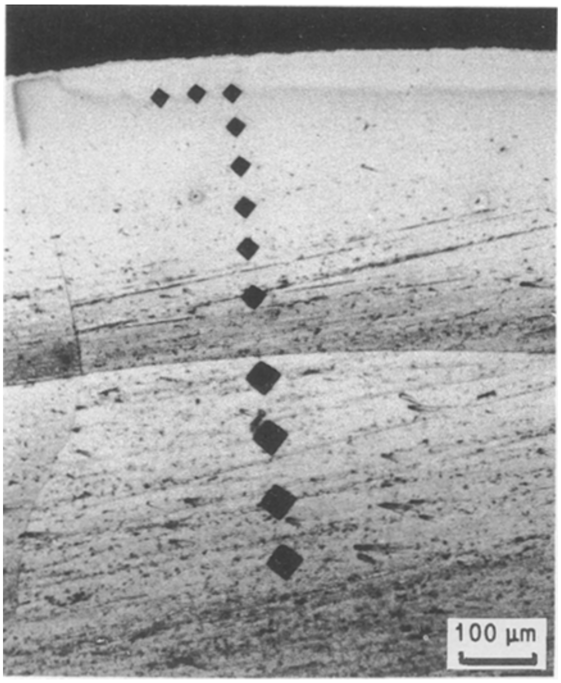

Figure 4 Optical micrograph and microhardness determinations on the cross-section of a siliconized sample for two hours at 1100 °C (total gas flow rate: 1.85 l h^{-1}; Ar 26.2 vol %; SiH_4 0.8 vol %; H_2 73 vol %).

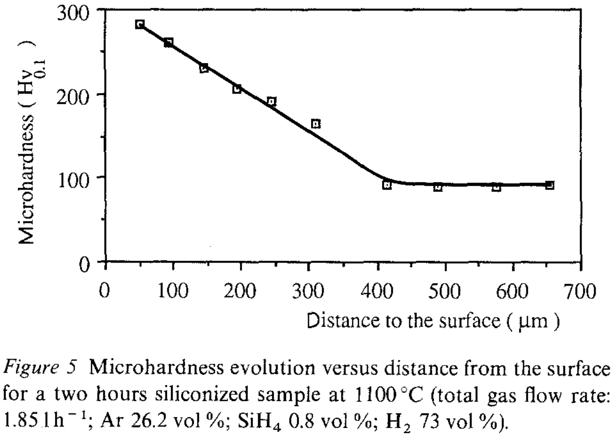

Figure 5 Microhardness evolution versus distance from the surface for a two hours siliconized sample at 1100 °C (total gas flow rate: 1.85 l h^{-1}; Ar 26.2 vol %; SiH_4 0.8 vol %; H_2 73 vol %).

spectroscopy are represented in Fig. 6, for a two hours siliconized sample at 1100 °C with the same vapour phase composition. The presence of ion $(FeSi)^+$ evidences the existence of stable chemical bondings between silicon and iron in the analysed layer.

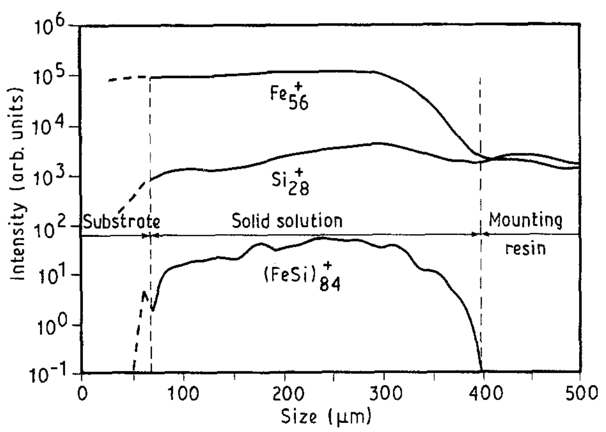

Figure 6 Distribution profiles of Si^+_{28}, Fe^+_{56} and $FeSi^+_{84}$ ionic species determined by SIMS (secondary ionic mass spectroscopy, with O_2^+ primary ions) for a two hours siliconized sample at 1100 °C (total gas flow rate: 1.85 l h^{-1}; Ar 26.2 vol %; SiH_4 0.8 vol %; H_2 73 vol %).

3.1.2. Effect of the SiH_4 flow rate

The effect of the siliconizing agent flow rate on the sample weight gain, for fixed experimental CVD conditions (vapour phase composition, temperature and duration of treatment) is summarized in Fig. 7. First, the weight gain increases with gas flow rate, then stabilizes for intermediary values before to slowly decrease for flow rate above 60 ml h^{-1}. The highest flow rates lead to the formation of a black, powdery, non-adherent deposit which break off from the substrate during the cooling down at the end of the treatment. At this point, weight gain determinations lose any signification. From X-ray diffraction analysis, it appears that the friable coating is mainly constituted of pure silicon or silicon rich iron-silicides such as FeSi and Fe_5Si_3.

3.1.3. Effect of hydrogen dilution of the Ar(97)-SiH_4 (3 vol %) mixture

The effect of dilution with hydrogen of the commercial Ar-SiH_4 mixture is shown in Fig. 8 for a CVD treatment of two hours at 1000 °C. The maximum weight gain is observed for a 30 to 70% dilution ratio.

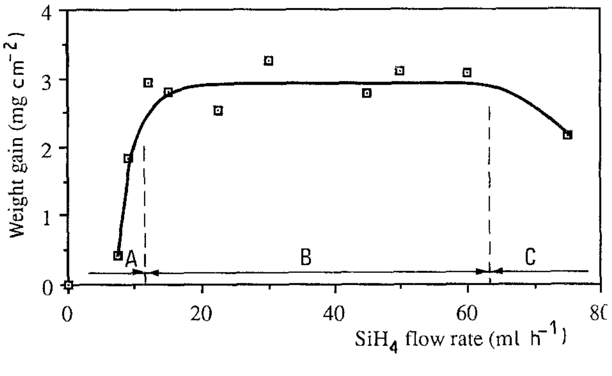

Figure 7 Effect of SiH_4 flow rate on the sample weight gain for a two hours siliconizing treatment at 1000 °C and a fixed composition of the vapour phase (Ar 26.2 vol %; SiH_4 0.8 vol %; H_2 73 vol %).

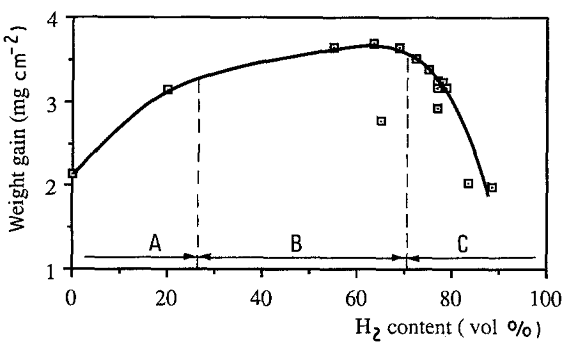

Figure 8 Effect of H_2 content in the vapour phase on the sample weight gain for a two hours siliconizing treatment at 1000 °C (initial gas composition: Ar 97 vol %; SiH_4 3; fixed SiH_4 flow rate: 0.4 l h^{-1}).

3.1.4. Effect of reaction temperature

The sample weight gains for various temperatures of two hours treatments are reported in Fig. 9 for a fixed vapour phase Ar–SiH_4–H_2 composition.

3.2. Ar–SiH_4–$SiCl_4$–H_2 mixture

The presence of $SiCl_4$ in the vapour phase entirely modifies the reaction process. As early as after the first few minutes of treatment, Fe_3Si (14.35 Si wt %) crystals develop on the surface of the treated samples, whatever the tested experimental conditions: duration and temperature of treatment as well as vapour phase composition.

The surface appearances of a siliconized Armco iron for 6 min at 1000 °C are reported in Fig 10. Successive strata of deposited layer growth from the remaining surface porosity. Such open porosity is still apparent with longer durations of treatment (Fig. 11), and is obviously related to the presence of $SiCl_4$ in the siliconizing atmosphere. Even a deposit initiated in Ar–SiH_4–H_2 mixture becomes porous if silicon tetrachloride is introduced afterwards in the vapour phase (Fig. 12). It is interesting to note that, when $SiCl_4$ is used, small sparkling crystals of Fe_3Si often nucleate onto the silica glass reactor wall, in the vicinity of the treated samples.

Figure 13 is relative to the distribution profile of silicon (wt %) into the coating, determined by microprobe analysis, after a sequential treatment at 1000 °C (55 min in Ar–SiH_4–H_2 mixture, then 5 min in

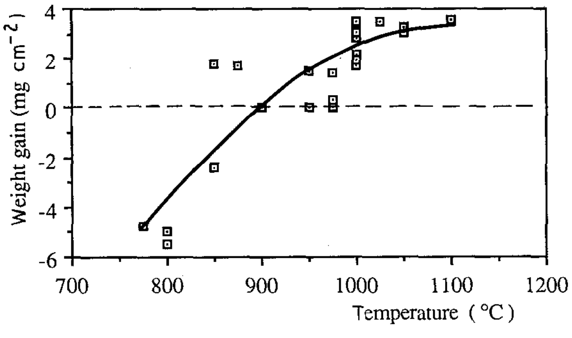

Figure 9 Effect of the reaction temperature on the sample weight gain (duration of treatment: 2h, total gas flow rate: 1.85 l h^{-1}; Ar 26.2 vol %; SiH_4 0.8 vol %; H_2 73 vol %).

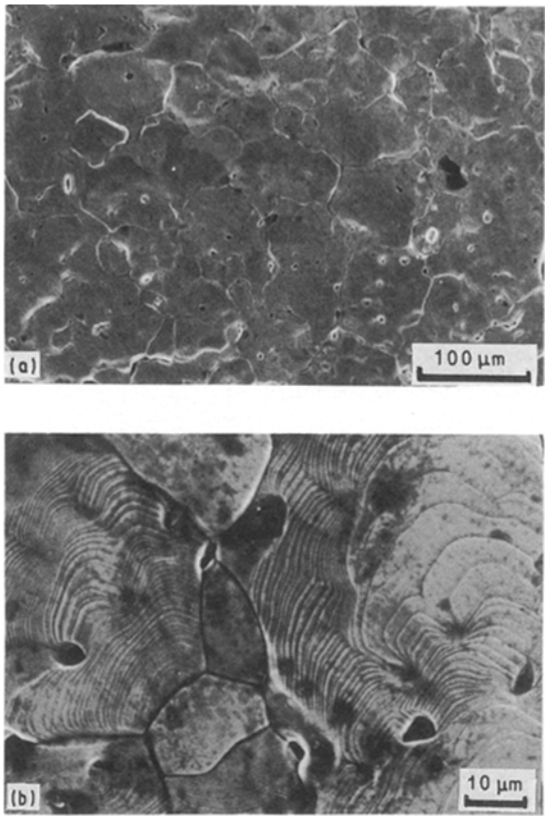

Figure 10a and b Surface appearances of a siliconized sample after 6 min of CVD treatment at 1000 °C (total gas flow rate: 1.85 l h^{-1}; Ar 21 vol %; SiH_4 0.6 vol %; $SiCl_4$ 20 vol %; H_2 58.4 vol %).

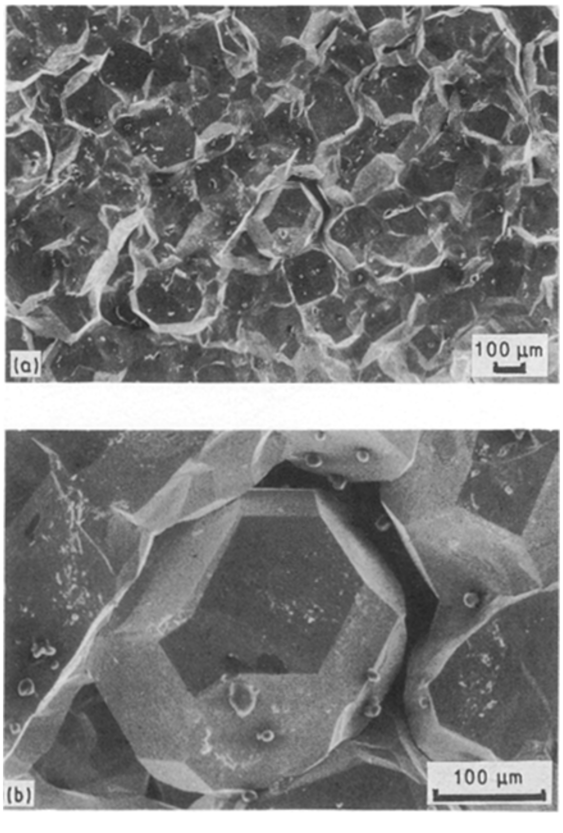

Figure 11a and b Surface appearances of a siliconized sample after 1 h of CVD treatment at 1000 °C (total gas flow rate: 1.85 l h^{-1}; Ar 21 vol %; SiH_4 0.6 vol %; $SiCl_4$ 20 vol %; H_2 58.4 vol %).

Table II: Diffusion coefficient of Fe in pure iron (self-diffusion) or in Fe_3Si and of Si in iron-silicon solid solution [14, 15]

T (°C)	D_{Fe} ($cm^2 s^{-1}$) in Fe_3Si	D_{Fe} ($cm^2 s^{-1}$) in pure iron	D_{Si} ($cm^2 s^{-1}$) in Fe-Si (7 at %) alloy	D_{Si} ($cm^2 s^{-1}$) in Fe-Si (21 at %) alloy
815	3.3×10^{-12}	7×10^{-12}	–	–
935	1.6×10^{-11}	8 to 9×10^{-11}	1×10^{-9}	5×10^{-9}

$Ar–SiH_4–SiCl_4–H_2$ mixture). The initial 7 Si wt % solid solution layer rapidly transforms into a richer deposit, the composition of which corresponding to Fe_3Si silicon content, but the structure becomes porous.

4. Discussion

4.1. $Ar–SiH_4–H_2$ mixture

4.1.1. Effect of the SiH_4 flow rate

As reported in Fig. 7, the sample weight gain increases with SiH_4 flow rate: in step A the gas phase transport of the reactant species and/or its dissociation in the gas phase, constitute the limiting processes of the overall reaction. In the stationary step B, the deposit kinetic may also be limited by the silane decomposition rate in the sample vicinity, but more probably by the solid diffusion rate of silicon and/or iron atoms in the growing layer. It becomes independent of the flow rate. In fact, according to literature data it appears that diffusion coefficients of silicon and iron are quite different in low silicon-iron alloys, as well as in iron silicide (Table II). The higher values for silicon atoms are in agreement with our own experimental results: we did not observe any noticeable Kirkendall effect which would eventually result from a faster iron atoms diffusion velocity.

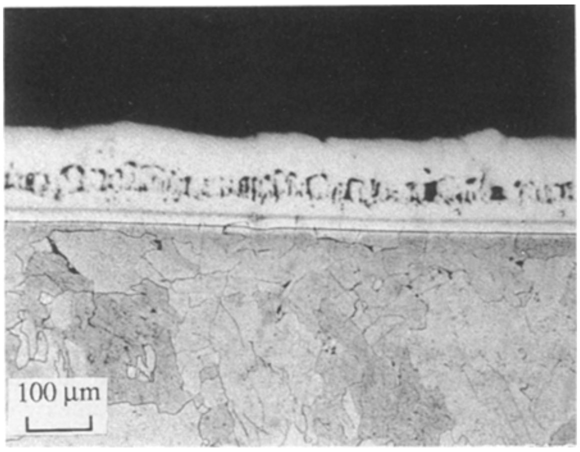

Figure 12 Optical micrograph of the cross-section of a siliconized sample after a sequential CVD treatment at 1000 °C; total gas flow rate: $1.85\ l\ h^{-1}$. (a) 55 min in Ar 26.2 vol %; SiH_4 0.8 vol %; H_2 73 vol %, (b) 5 min in Ar 21 vol %; SiH_4 0.6 vol %; $SiCl_4$ 20 vol %; H_2 58.4 vol %.

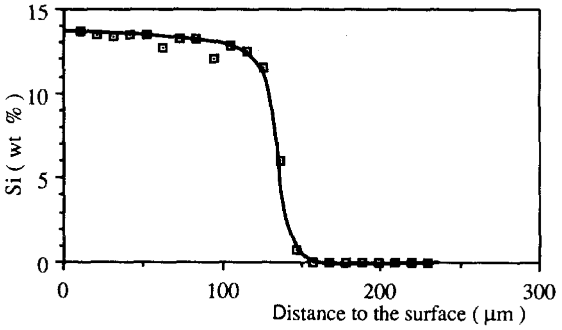

Figure 13 Distribution profile of silicon into the coating after a sequential CVD treatment at 1000 °C (same experimental conditions as Fig. 12).

As previously mentioned, the apparent weight gain evolution in step C is not related to the kinetic of the reaction process, but is due to the formation of non-adherent deposit of pure silicon powder or flakey and friable silicon rich iron-silicides.

4.1.2. Effect of vapour phase composition

The layer growth rate when using $Ar–SiH_4–H_2$ mixture may also be controlled by the dissociation rate of silane, as evinced in Fig. 8. In fact, the vapour phase dilution with hydrogen slows down the dissociation of silane according to reaction

$$SiH_4 \underset{2}{\overset{1}{\leftrightarrows}} Si + 2H_2$$

Alternatively, the use of argon as diluting agent for a given total vapour pressure, leads to the shift of the reaction towards direction 2.

For a low level of hydrogen dilution (step A), the silane dissociation rate is too fast, and silicon deposes mainly on silica glass reactor before the siliconizing agent could reach the sample. In step B, the reaction equilibrium is sufficiently shifted in direction 1 for slowing down the silane decomposition rate on the reactor wall. Most of the deposit occurs on the sample and the growth rate-determining step is again the diffusion of silicon atoms into the siliconized layer. In step C the dilution is too important, thus decreasing the silane content in the vapour phase and its reactivity: the weight gain rapidly declines with increasing hydrogen dilution.

4.1.3. Effect of reaction temperature

Whatever the reaction temperature, the decomposition of silane leads to deposit of silicon on the substrate. Yet below 850 °C we do not observe a weight gain, but a weight loss of the samples during the siliconizing treatment. This apparent contradiction may be explained if we take into account the evolution

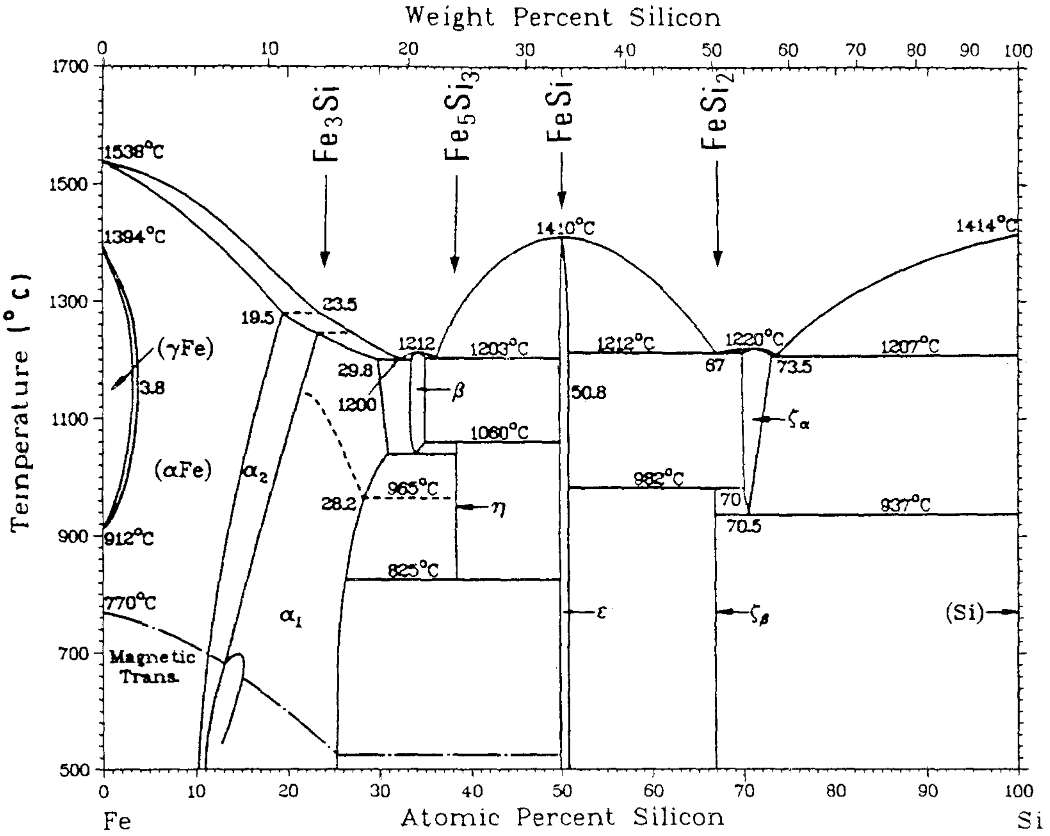

Figure 14 Fe-Si equilibrium phase diagram [19].

versus time of the solid Si/Fe diffusion system which appears on the surface of treated specimens at the beginning of the CVD process. For lower tested temperatures of treatment, the diffusion velocity of Si atoms throughout the successive layers of silicon-rich silicides (formed according to Si-Fe phase diagram represented in Fig. 14) is too low to promote a thick layer of silicon-iron solid solution in a few hours of treatment. Iron silicides layers are very brittle and non-adherent; they break off and finally sample loses weight.

Above 910 °C f c c-iron sample surface progressively transforms into b c c lattice during the siliconizing treatment due to the increasing amounts of silicon which is a ferrite former (Fig. 14). In less compact b c c lattice compared to f c c austenitic structure, the velocity of diffusing species is more important. Furthermore higher temperatures and consequently larger silicon diffusion coefficients in the substrate allow the formation of thick layers of iron-silicon solid solution (Fig. 2 and 4). The coatings are always adherent, except for excessive flow rate of SiH_4 which may cause the deposit of flakey silicides. For low or moderate flow rate, only a fine silicide layer develops onto the outer surface of the solid solution (Fig. 2).

4.2. Ar–SiH_4–$SiCl_4$–H_2 mixture

The use of chlorinated siliconizing agent ($SiCl_4$ in our case) induces the immediate formation of Fe_3Si, whatever the temperature. In similar conditions, Motojima [13] observed on Fe substrates the successive formation of Fe_3Si/FeSi/$FeSi_2$, when siliconizing iron plates with Si_2Cl_6 as source silicon. He also observed the formation of many voids or cavities in the iron plate and siliconized layer interface, attributed to the Kirkendall effect resulting from the difference between the diffusion velocity of Si and Fe atoms in the surface layer, that is in some contradiction with the diffusion coefficient values reported in the literature (Table II). We did not observe such important Kirkendall effect with $SiCl_4$ as reacting agent, but an open porosity which allows easy formation and departure of $FeCl_2$. Ferrous chloride reacts with previously formed silicon dichloride, the existence of the latter having already been noticed by authors studying iron siliconizing in $SiCl_4$–H_2 vapour phase [5, 10]. If Reactions 1 and 2 have often been taken into account, Reaction 3 to our knowledge has never been mentioned in previous work. Yet the formation of Fe_3Si crystals in the vapour phase outside the sample surface confirms the possibility of its nucleation without solid iron support and the large value ($-417\ kJ\,mol^{-1}$) of the free energy of Fe_3Si formation, calculated at 1000 °C from literature thermodynamic data [16–18] according to Reaction 3, is another indication of the strong probability of that reaction.

$$SiCl_4(g) + H_2(g) \leftrightarrows SiCl_2(g) + 2\,HCl(g) \quad (1)$$

$$Fe(s) + 2\,HCl(g) \leftrightarrows FeCl_2(g) + H_2(g) \quad (2)$$

$$3FeCl_2(g) + 5\,SiCl_2(g) \leftrightarrows Fe_3Si(s) + 4\,SiCl_4(g) \quad (3)$$

By using Eriksson computer program [20] it can be shown that silicon dichloride initially formed (Reaction 1) entirely reacts with volatile iron dichloride coming out from the open porosity, promoting the

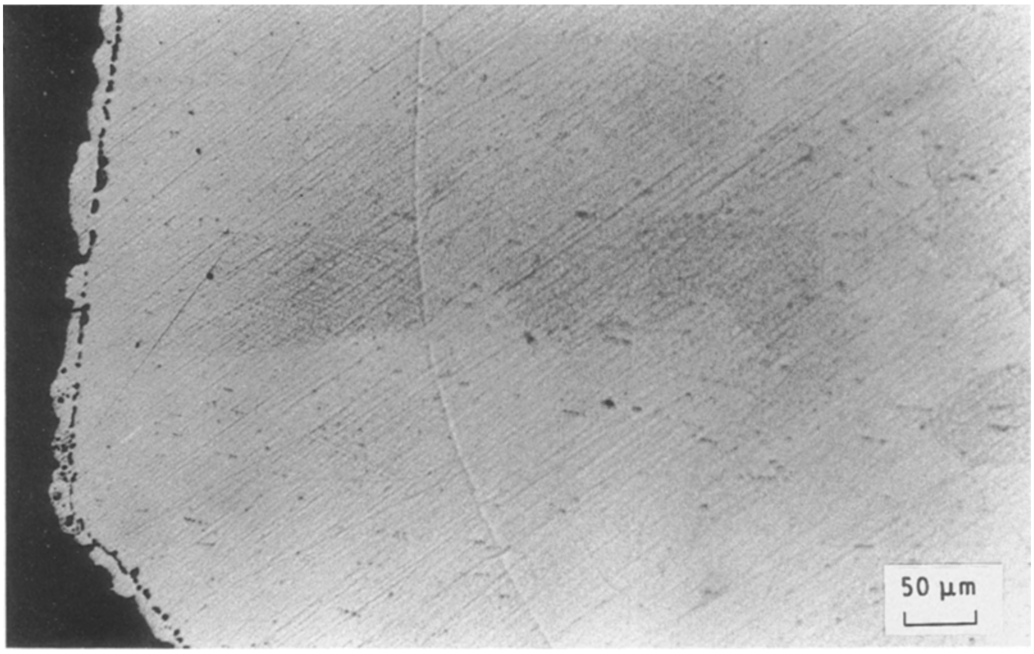

Figure 15 Optical micrograph of the cross-section of a coating obtained on Armco iron after a silicon solid phase diffusion treatment of 24 h at 1000 °C.

growth of observed Fe_3Si strata-shape layers around each pore (Figs 10 and 11). In the case of siliconizing without chlorinated silicon source, such as $Ar–SiH_4–H_2$ vapour phase, Reaction 3 is impossible and silane thermal dissociation can only induce physical deposition and growth of pure silicon crystals. Due to high temperature of CVD treatment and fast resulting diffusion velocity of silicon atoms into the substrate (with subsequent slower back diffusion of iron atoms towards the outer surface), only silicon-iron solid solution forms together with some brittle and non-adherent silicides if the rate of silane pyrolysis is too high, that means for important flow rates. In order to confirm that hypothesis, we realized some experiments without vapour silicon source, but with possible silicon surface enrichment of the sample through solid phase diffusion. The Armco iron samples were positioned at room temperature in a ceramic box containing high purity silicon powder, then treated at 1000 °C for various durations of treatment under a steady flow of hydrogen to avoid any oxidation.

Figure 15 corresponds to a coating formed after 24 h at 1000 °C, and illustrates the similarity at least for the obtained layers, between the two types of treatment: CVD in silane vapour phase or with solid diffusion from surrounding silicon powder. In both case, a coating of silicon-iron solid solution develops under a thin layer of non-adherent iron silicide. As expected, the sole difference is a much slower coating growth rate for the solid phase diffusion treatment.

5. Conclusion

The gaseous phase composition plays a major role on the nature and the structure of the coating formed when siliconizing Armco iron.

With $Ar–SiH_4–H_2$ vapour phase, the deposition of silicon powder by pyrolytic decomposition of silane, leads by diffusion of the silicon into the substrate and according to the equilibrium phase diagram, to the formation of iron silicides which are non adherent. Yet the growth of a thick layer of an iron-silicon solid solution containing up to 6 wt % Si occurs very rapidly if the treatment temperature is high enough. That layer is very adherent and non porous. Flow rate and dilution of the gas mixture with hydrogen, as well as reaction temperature have an important effect on the relative weight gain of the samples during the siliconizing treatment.

The presence of chlorosilane in the gaseous phase entirely modifies the reaction process. For instance, the use of $Ar–SiH_4–SiCl_4–H_2$ mixture leads to the immediate nucleation of Fe_3Si, the growth of which occurring from and around the open porosity of the coating. From our experimental observations and in agreement with thermodynamic data, it appears that the Fe_3Si formation results from the reaction between silicon chloride and iron dichloride formed during the CVD process.

Acknowledgments

This work was financially supported by the Department of Material Study, Electricité de France, Les Renardières, 77250 Moret-sur-Loing.

References

1. G. H. MEIER, in Proceedings of the Material Research Society Symposium **81** (1987) 443.
2. A. ATKINSON, *Corrosion Science* **22** (1982) 87.
3. *Idem, ibid.* **22** (1982) 347.
4. P. T. MOSELEY, G. TAPPIN and J. C. RIVIERE, *ibid.* **22** (1982) 69.
5. Y. CETRE, in "Etude du comportement à la corrosion de divers matériaux métalliques dans l'acide sulfurique concentré chaud", Doctoral thesis, Lyon (1985) no. IDI1 8524.

6. B. J. SALDANHA and M. A. STREICHER, *Mat. Perform.* **25** (1986) 37.
7. K. SUGIYAMA and T. NAGASHIMA, *Kinzoku Hyomen Gijutsu* **22** (1988) 388.
8. Y. CETRE, S. AUDISIO and H. MAZILLE in Proceedings of the 10th International Congress on Metallic Corrosion, Madras, (November 1987) p. 1151.
9. A. ABBA, A. GALERIE and M. CAILLET, *Materials Chemistry* **5** (1980) 147.
10. S. AUDISIO, in "Etude de l'interaction surface métallique-phase gazeuse: Fe–$SiCl_4$–Ar. Propriétés des couches épitaxiques obtenues", Doctoral thesis, Lyon (1968) no. 503.
11. H. ITOH, K. KATO and K. SUGIYAMA, *J. Mat. Sci.* **21** (1986) 751.
12. A. R. NICOLL, U. V. HILDEBRAND and G. WAHL, *Thin Solid Films* **64** (1979) 321.
13. S. MOTOJIMA, T. HATTORI and K. YAMAGUCHI *J. Crystal Growth* **85** (1987) 309.
14. S. AUDISIO and P. GUIRALDENQ, in Proceedings of "Euro CVD Seventh Symp." Perpignan (June 1989) p. C5–455.
15. H. MITANI, M. ONOISHI and T. SHIKANO, *Nippon Kinzoku Gakkai-shi* **30** (1966) 56.
16. D. R. STULL and H. PROPHET, in "Janaf Thermochem. Tables", 2nd edn, NSRDS-NBS **37** (1971).
17. I. BARIN, O. KNACKE and O. KUBASCHEWSKI, in "Thermochemical Properties of Inorganic Substances", (Springer-Verlag, Berlin, 1977).
18. T. G. CHART, in "Données Thermochimiques pour la Sidérurgie", Rapport final CECA no. 7210 CA/3/303, edited by IRSID (France) PCM-RE.852 (November 1981).
19. Th. B. MASSALSKI, in "Binary Alloy Phase Diagrams", ASM Public, Ohio 44073, **2** (1986) 1108.
20. G. ERIKSSON and E. ROSE'N, *Acta Scripta* **4** (1973) 193.

Received 11 June
and accepted 26 June 1990